621.181.6

Paper No. 143-20

Pressure Drops in Supercritical Boilers*

(1st Report. Static Characteristics of Friction Pressure Drop)

By Tadashi SAKAGUCHI** Koji AKAGAWA**

Mamoru OZAWA*** Kiyoshi AWAI****

Yukio MIYAMOTO***** Takafumi ORIGANE******

Static and dynamic characteristics of pressure drop in supercritical pressure boilers were studied. In this paper, experimental results of static pressure drop of CO_2 at supercritical and relatively high subcritical pressures in a heated test tube were presented, and effects of various factors such as flow rate, heat flux, inlet temperature, and pressure were discussed. The calculated results by numerical integration using the friction coefficient of single phase flow agreed with the experimental results. The experimental results were well correlated by the dimensionless expression of pressure drop previously reported. This means that the results obtained by this CO_2 experiment will be also applicable to the case of working fluid of H_2O. Mean friction coefficients of supercritical fluid in the whole tube length were shown and an empirical equation of the coefficient for the heat flux was proposed.

1. Introduction

Recent development in supercritical pressure power plants requires more precise information on the characteristics of heat transfer and pressure drop of the working medium in steam generator at the supercritical pressure. Static and dynamic behaviors of pressure drop are one of the important factors in designing steam generating tubes of supercritical boilers. Many investigations on the pressure drop in the low pressure steam generator have been conducted, but few investigations have been made on the pressure drop in the supercritical pressure region and subcritical pressure region near supercritical pressure.

This series of reports presents experimental and theoretical results of pressure drop in the supercritical and subcritical pressure regions of the steam generating tubes. In this first report the static characteristics of friction pressure drop in supercritical and near critical pressure regions are presented and in the following reports the experimental results and the theoretical analysis of dynamic characteristics will be reported.

Carbon Dioxide is selected as the working medium in this study for the following reasons: (1) High cycle efficiency can be obtained by CO_2 condensing cycle as reported by Angelino[1]. (2) The critical pressure of CO_2 is relatively low, 75.3ata, and the critical temperature is low, 31.04 °c. (3) CO_2 is chemically stable and harmless. (4) Experimental results for CO_2 can be applied to predict the characteristics for high pressure steam by the authors' method.

Pressure drops in steam generating tubes of supercritical pressure boilers are large compared with the system pressure. Then the purpose of this study is to make clear the characteristics of large pressure drop in a long heating tube. Therefore, the experiment is conducted with the condition of maximum pressure drop of 30 kg/cm^2 for the exit pressure of 80 ata. The characteristics of friction pressure drop with respect to heat flux, inlet temperature, and system pressure are obtained experimentally and are compared with the numerical analysis of authors' and with other correlations previously reported.

2. Experimental apparatus and Procedure

A schematic diagram of the apparatus is shown in Fig.1. Liquefied CO_2 supplied from a vessel (13) is circulated by a reciprocating pump (1) with a R.P.M. regulator (2) through a filter (4), preheater (5), flow meter (7), test section (8), and condenser (10). The pressure at the exit of the test section is controlled by the exit valve (9). Flow fluctuation is eliminated by an accumulator (3). Flow rate is controlled by regulating the pump speed and the flow control

* Received 17th June, 1974.

** Professor, Faculty of Engineering, Kobe University.

*** Research Assistant, Faculty of Engineering, Osaka University.

**** Engineer, Sumitomo Shipbuilding and Machinery Co., Ltd.

***** Engineer, Daikin Kogyo Co., Ltd.

****** Engineer, Kawasaki Heavy Industry Co., Ltd.

valve (6). The flow rate is calculated from the pressure drop in a helical tube type flow meter (7) and the pressure drop is measured by a differential pressure transducer (21), strain amplifier (20), DC amplifier (19), and recording oscillograph (18). The calibration curve of flow rate is obtained by a water test run using relation between the friction coefficient and the Dean number $D_e=R_e(d/D)^{0.5}$. The pressure at each location is measured by Bourdon tube pressure gauges. The pressure drop in the test section is measured by two pressure transducers (23) and a bridge circuit (22), and is recorded by an oscillograph (18) through a strain amplifier (20) and a DC amplifier (19). Test section inlet temperature is controlled by a voltage regulator (14) and measured by a C-A thermocouple and a digital voltmeter (32). Test section exit temperature is measured by a similar method as the inlet temperature. (31) is a cold junction for thermocouples. Tube wall temperatures along the test section are measured by 12 C-A thermocouples and a temperature indicator (30). The test tube is heated uniformly by alternating current of voltage lower than 20 v transformed by a voltage regulator (26) and a trnasformer (27). The electric power is measured by a current transformer (28) and a wattmeter (29).

The detail of the test section is shown in Fig.2. The test section is constructed of SUS304 tube with 3.95 mm I.D., 7.0 mm O.D., 28.3 m total length, 246 mm coil diameter and 1.35 m heigth. Electric power is supplied to the test section from 4 copper terminals which divided the test tube into three portions of equal length, and the test tube is thermally insulated by glasswool. Frition coefficient measured in turbulent region in a straight section which is constructed of the same tube as the helical test section coincides with Blasius' equation.

The friction coefficient λ_c in the test section measured for single phase flow of water is shown in Fig.3. In the figure the ratio of λ_c to λ_{SL} is plotted against Dean number, where the friction coefficient λ_{SL} is calculated by the equation $\lambda_{SL}=64/R_e$. The experimental results in laminar flow region agree well with White's curve [2] and that in turbulent flow region is a little higher than Ito's equation [3]. The latter may be due to the resistance by the welded connections between element tubes in the test section. The experimental results are expressed by an empirical equation

$$\lambda_c/\lambda_{SL}=0.008\,326D_e^{0.906\,9} \quad \cdots\cdots\cdots\cdots\cdots\cdots (1)$$

in turbulent flow region where the Dean number is higher than the critical value of Ito's equation [3] $D_{ecr}=2(d/D)^{0.82}\times10^4$.

All experimental data are obtained by changing the flow rate stepwise at a constant condition of exit pressure, inlet temperature, and heat input, and the same procedures are repeated under different exit pressures, inlet temperatures, and heat inputs. Thus, the friction pressure drop versus the flow rate curves are obtained for various values of parameters. From these curves the characteristics of the friction pressure drop are investigated. In order to check the inner condition of the test tube, the pressure drop under non-heated condition is measured before and after each test run to confirm the condition being unchanged.

Experimental ranges are as follows: Exit pressure P_e=60~80 ata, heat flux Q=0~1.3×10^4 kcal/m^{2}h, inlet temperature T_i=12~28 °c, flow rate 472~4700 kg/m^{2}s.

3. Friction pressure drop in heated tube

Friction pressure drop in heated tube ΔP_f is obtained by

$$\Delta P_f=\Delta P-(\Delta P_a+\Delta P_h)+H_m\gamma_0 \quad , \quad \cdots\cdots\cdots\cdots (2)$$

where ΔP is the differential pressure measured in the test tube, ΔP_a the acceleration pressure drop, ΔP_h the gravitational pressure drop, H_m the height between the inlet and exit pressure taps, and γ_0 the mean specific weight of CO_2 in the connection

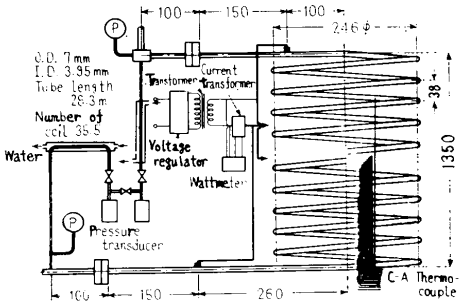

Fig.2 Details of test section

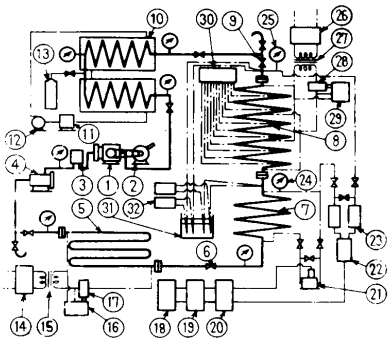

Fig.1 Experimental apparatus

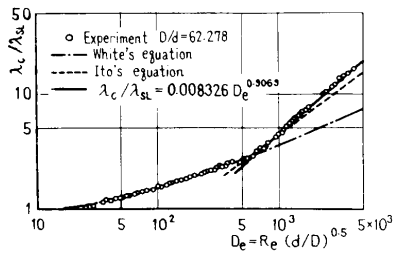

Fig.3 Friction coefficient of test tube

tube from the pressure tap to pressure transducers. In these experiments the values of ΔP_a and ΔP_h are very small compared with ΔP_f and the value of $(H_m\gamma_o-\Delta P_a-\Delta P_h)/\Delta P_f$ is less than 1 %. Therefore the measured values of ΔP can be considered the friction pressure drop in these experiments.

3.1 Experimental results of friction pressure drop

In Figs.4, 5, 6, 7, and 8 are shown the experimental results at various conditions of exit pressure P_e=80, 65, 60 ata, inlet temperature T_i=12, 22, 25, 28 °c, heat flux Q=0~1.3×10^{4}kcal/m^{2}h. As the critical pressure of CO_2 is 75.3 ata, the reduced pressures P/P_{cr} of these runs are 1.06, 0.863, and 0.797, therefore these values correspond to the exit pressure of 240, 195, and 179 ata for water. The relation between friction pressure drop and flow rate in the case P_e =80 ata is shown in Fig.4 for various values of T_i and Q. For the case of Q=0 kcal/m^{2}h ΔP_f increases monotonously as a curve of second degree. The higher the heat flux, the higher the friction pressure drop, and when the value of Q is relatively high, the curve of ΔP_f has a point of inflexion like a curve of third degree. In Fig.5 the effect of inlet temperature on friction pressure drop at P_e=80 ata is shown. Friction pressure drop increases with the inlet temperature for any value of heat flux, because of the increase of specific volume of CO_2. The curve of ΔP_f-G has a point of inflexion at low flow rates for relatively high heat flux. This is explained by the following reason.

Friction pressure drop in the whole length L_T is obtained by the equation

$$\Delta P_f=\frac{1}{2gd}\left(\frac{G}{F}\right)^2\int_0^{L_T}\lambda v dL\ , \quad \cdots\cdots\cdots\cdots (3)$$

where v is the specific volume at a location L, λ is the friction coefficient at L, and F is the cross sectional area of the test tube. Here, the fluid flow in supercritical pressure region can be considered a single phase flow, so v can be determined uniquely without taking account of steam quality or slip ratio in two phase flow, and λ is determined in the same manner as in the single phase flow, though the value is affected by the density and viscosity distributions in the cross section. The specific volume in supercritical pressure increases approximately linearly with the enthalpy as shown in Fig.9, and the slope in the range higher than the pseudo-critical point is far larger than that in the lower region. The upstream region from the pseudo-critical point is called a preheated region and the downstream region is called a superheated region. Equation (3) is expressed with the preheated length L_1 as follows:

$$\Delta P_f=\frac{L_T}{2gd}\left(\frac{G}{F}\right)^2\left[\frac{1}{L_T}\int_0^{L_1}\lambda v dL+\frac{1}{L_T}\int_{L_1}^{L_T}\lambda v dL\right]\ . \quad \cdots\cdots (4)$$

In the case of higher flow rate L_T is equal to L_1, so ΔP_f is equal to the first term in the right hand side of the above equation. The change of specific volume is so small that only the effect of flow rate on pressure drop is dominant. In the case of lower flow rate, the length L_1 decreases and L_2 increases and also the change of v in the second term is large, therefore the friction pressure drop of the sum of two terms has a point of inflexion on the curve of ΔP_f-G.

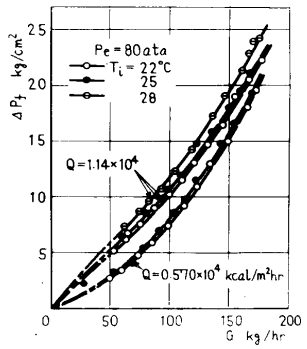

Fig.5 Friction pressure drop

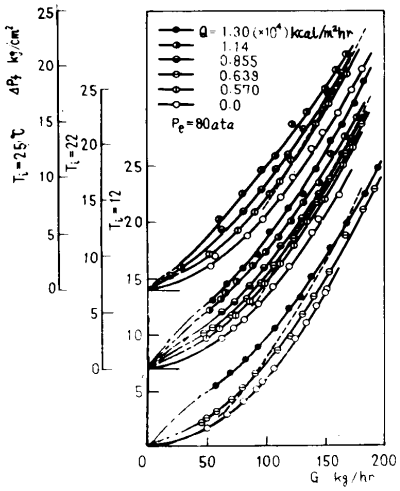

Fig.4 Friction pressure drop

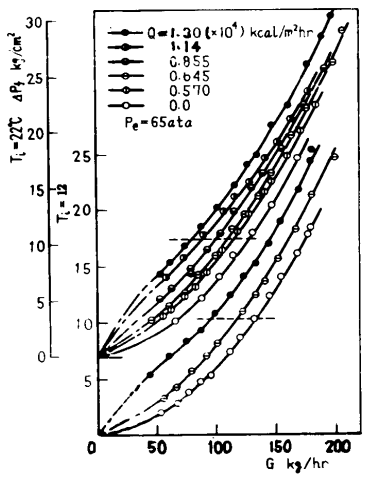

Fig.6 Friction pressure drop

The broken line in Fig.4 is the locus where the exit of the test section is at the pseudo-critical condition. At the right hand region of that line, all the test tube length is in the preheated region, and the left hand region the test tube is constructed of the preheated and superheated regions. In Figs.6 and 7 are shown the friction pressure drop - flow rate characteristics at P_e=65 ata, T_i=12, 22 °c, and Q=0~1.3×10^4 kcal/m^2h. In these case the exit pressure is below the critical pressure, and when the friction pressure drop is larger than 10.3 kg/cm^2, the pressure at the inlet of the test section is higher than the critical pressure, 75.3 ata. The boundary is shown by the broken lines in the figures. ΔP_f increases with the inlet temperature and heat flux. The friction pressure drop in the region above the broken line increases monotonously with the flow rate, because the change of specific volume due to evaporation is very small at this subcritical high pressure and only the effect of flow rate dominates. In the lower region of the broken line ΔP_f-G curve apparently has a point of inflexion at high heat flux and low flow rate for the same reason as mentioned above.

Figure 8 shows the effect of the exit pressure on ΔP_f at T_i=22 °c. The value of ΔP_f increases with a decrease of the exit pressure at each value of heat flux; this mainly due to the increase of specific volume with the decrease of pressure.

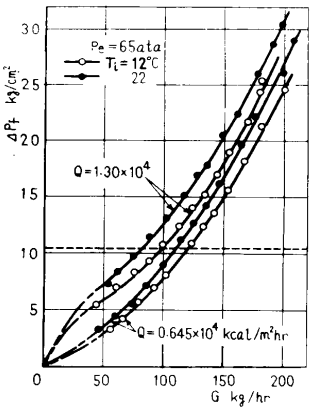

Fig.7 Friction pressure drop

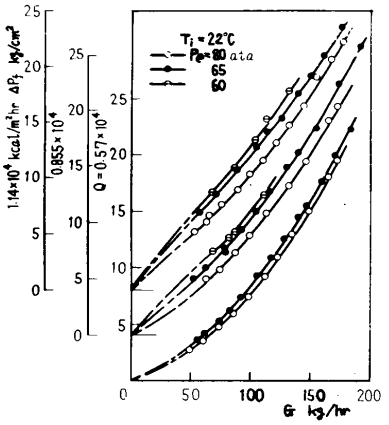

Fig.8 Friction pressure drop

3.2 Numerical analysis of friction pressure drop and comparison with experimental results

The density, the dynamic viscosity, and the specific heat of the fluid at supercritical pressure change abruptly in the pseudo-critical region, therefore the variation of these properties along the tube or in the boundary layer inside tube will affect the pressure drop. But the variation of these properties in a boundary layer is not taken into account in this report and the fluid at supercritical pressure is assumed as a homogeneous fluid, thus the friction coefficient in a straight tube can be calculated by Blasius' equation using the properties at the mean enthalpy in the cross section. Also, the friction coefficient in the test section is calculated by the experimental equation (1) which is similar to Ito's equation [3]. The variation of the velocity and friction coefficient with the enthalpy and the static pressure along the test tube length results in the change of the pressure gradient at the local point in the test section. So it is necessary to integrate the local value of the pressure gradient along the test tube in order to get an exact value of the total pressure drop. The calculation is conducted numerically by a digital computer.

Momentum equation for a test tube segment in Fig.10 is given by

$$-\frac{dP}{dL}=\frac{G^2}{gF^2}\left(\frac{dv}{dL}\right)+\frac{\sin\theta}{V}+\lambda\frac{1}{2gd}\left(\frac{G}{F}\right)^2 v \quad \cdots\cdots\cdots(5)$$

wherw θ is the angle between the tube axis and the horizontal plane; g is the gravitational acceleration. The value of enthalpy i_{j-1} at the exit of segment j can be obtained from the flow rate, the heat input, and the enthalpy at the tube inlet as follows:

$$i_{j-1}=i_i+Q_T(N-j+1)/G/N \quad \cdots\cdots\cdots\cdots(6)$$

Specific volume v_{j-1} and kinetic viscosity

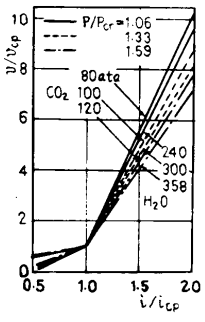

Fig.9 Approximate relation between specific volume and enthalpy

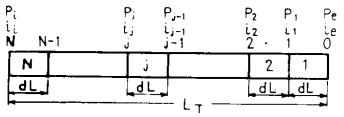

Fig.10 Model of heated tube

v_{j-1} at point j-1 are determined by using enthalpy i_{j-1} and pressure P_{j-1} from a steam table. The specific volume and the kinetic viscosity for the segment j are assumed to be approximately equal to v_{j-1} and ν_{j-1} respectively , then from Eq.(5) the friction pressure drop, the acceleration pressure drop, and the gravitational pressure drop at the segment j are expressed by Eqs.7, 8, and 9 respectively.

$$\delta P_{fj}=\lambda_j\frac{dL}{2gd}\left(\frac{G}{F}\right)^2 v_{j-1} \quad , \cdots\cdots\cdots (7)$$

$$\delta P_{aj}=\frac{1}{g}\left(\frac{G}{F}\right)^2 (v_{j-2}-v_{j-1}) , \cdots\cdots\cdots (8)$$

$$\delta P_{hj}=\frac{dL}{v_{j-1}}\sin\theta \quad , \cdots\cdots\cdots (9)$$

where λ_j is the friction coefficient for the segment j and is calculated from v_{j-1}, ν_{j-1}, and Eq.(1). The sum δP_j of Eqs.(7), (8), and (9) gives the pressure drop at the segment j, then the inlet pressure in segment j is given by

$$P_j=P_{j-1}+\delta P_j \quad . \cdots\cdots\cdots (10)$$

Pressure drop at segment j+1 is calculated by using P_j and i_j in the same manner. Thus the pressure drop along the whole test tube can be obtained by repeating these calculations from the exit of the tube to the inlet. These calculations are conducted with the number of segments N=30 by numerical integration.

The comparison of the calculated values and the experimental ones is shown in Fig.11. The calculated values at Q=0 kcal/m^{2}h agree well with the experimental ones. For the case of the heating experiment, the calculated values agree approximately with the experimental ones but are little higher than the experimental ones. The reason may be that the estimated friction coefficient determined from the mean enthalpy in the cross section is smaller than the actual friction coefficient, because the temperature in the boundary layer is near the pseudo-critical temperature and the value of viscosity becomes lower and also the velocity profile is not the same as in homogeneous fluid [4].

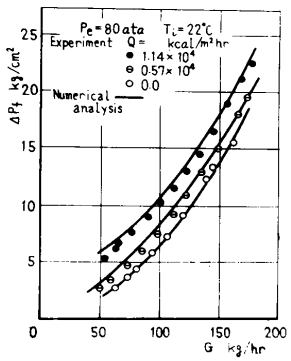

Fig.11 Comparison between calculated and experimental values of friction pressure drop

3.3 Mean friction coefficient of fluid in supercritical pressure region

It is desirable to calculate the pressure drop with a simpler method using the mean values of the friction coefficient. Assuming that the friction coefficient λ_{ex} is constant along the tube and the mean specific volume in preheated and superheated region is approximated by $v_1=(v_i+v_{pcr})/2$ and $v_2=(v_{pcr}+v_e)/2$ respectively, then λ_{ex} is expressed by

$$\lambda_{ex}=\Delta P_f\Big/\left[\frac{L_T}{2gd}\left(\frac{G}{F}\right)^2\left(\frac{v_i+v_{pcr}}{2}\frac{L_1}{L_T}+\frac{v_{pcr}+v_e}{2}\frac{L_1}{L_T}\right)\right], \cdots (11)$$

where the values of L_1, L_2 are determined by the equations $L_1=(i_{pcr}-i_i)/(i_e-i_i)$, $L_2=L_T-L_1$, in which pseudo-critical enthalpy i_{pcr} is assumed to be determined from the exit pressure, and v_i and v_e are the specific volumes at the tube inlet and exit respectively, and v_{pcr} the pseudo-critical specific volume determined from i_{pcr}. λ_{ex} is expressed by a ratio of an assumed friction coefficient λ_m which is calculated from Eq.(1) using the exit pressure and the mean enthalpy and specific volume.

In Fig.12, the ratio of λ_{ex} to λ_m is shown for various heat fluxes Q against the mean Reynolds number $R_{em}=Gdv_m/(F\nu_m)$, where v_m and ν_m are mean values of specific volume and kinetic viscosity respectively. The ratio λ_{ex}/λ_m is about 1.0 at Q=0 kcal/m^{2}h and has a tendency to decrease with an increase of heat flux, and Reynolds number does not affect the ratio. The relation between λ_{ex}/λ_m and Q for these experiments is given by an empirical formula as shown in Fig.13

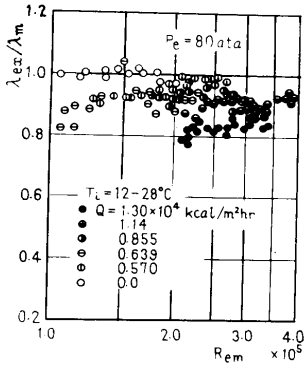

Fig.12 Mean friction coefficient

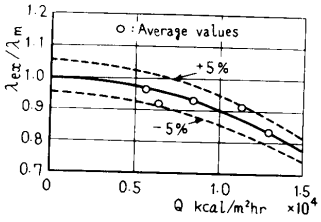

Fig.13 Mean friction coefficient

$$\lambda_{ex}/\lambda_m = 1.0 - 0.1(Q/10^4)^2 \quad \cdots\cdots\cdots\cdots (12)$$

The experimental results of λ_{ex}/λ_m agree with Eq.(12) within an error of ±5 %.

3.4 Friction pressure drop ratio in subcritical pressure region

The friction pressure drop in an evaporating region is given by

$$\Delta P_v = \Delta P_f - \Delta P_c \quad , \quad \cdots\cdots\cdots\cdots (13)$$

where ΔP_c is the friction pressure drop in the preheated region. Here, ΔP_c is assumed to be given by

$$\Delta P_c = \lambda' \frac{L_T}{2gd}\left(\frac{i'-i_i}{i_e-i_i}\right)\left(\frac{G}{F}\right)^2 \frac{v_i+v'}{2} \quad , \quad \cdots\cdots (14)$$

where the friction coefficient λ' is approximated by that for saturated liquid, the specific volume is approximated by $(v_i+v')/2$ and also the saturated liquid enthalpy for a value equal to the tube exit pressure. Then the friction pressure drop ratio $\Delta P_v/\Delta P_\ell$ is defined as the ratio of friction pressure drop at the evaporating region to an imaginary friction pressure drop of single phase flow in saturated liquid condition, which is given by

$$\Delta P_l = \lambda' \frac{L_T}{2gd}\left(\frac{i_e-i'}{i_e-i_i}\right)\left(\frac{G}{F}\right)^2 v' \quad . \quad \cdots\cdots\cdots (15)$$

The expression of $\Delta P_v/\Delta P_\ell$ was used in correlations for steam-water two-phase flow and the correlation curves for various pressures were proposed by Martinelli-Nelson [5] and Thom [6].

The relation between $\Delta P_v/\Delta P_\ell$ and exit quality $x_e=(i_e-i')/(i''-i')$ is shown in Fig. 14 for various T_i and Q. It is seen that $\Delta P_v/\Delta P_\ell$ is independent of the heat flux and inlet temperature and can be expressed by an empirical equation

$$\Delta P_v/\Delta P_l = 0.54 x_e + 1.0 \quad . \quad \cdots\cdots\cdots\cdots (16)$$

In order to compare the present results with those in water, Thom's curves for water at 195 ata, $(P/P_{cr}=0.863)$ and 211 ata $(P/P_{cr}=0.935)$ are cited in the figure. These pressures correspond to 65 ata and 70.4 ata for CO_2 respectively. These exprimental results for CO_2 are for the exit pressure of 65 ata, so the pressure at the inlet is 95 ata to 68 ata. Therefore, these data refer to the region between Thom's curve for 195 ata and the horizontal line, that is $\Delta P_v/\Delta P_\ell=1.0$. Consequently, it can be said that these experimental results approximately agree with Thom's correlation which is modified for CO_2.

4. Dimensionless expression of friction pressure drop

Generalized expressions for friction, acceleration, and gravitational pressure drops were proposed in the authors' previous report [7], and the effects of flow rate, inlet temperature, heat flux, and pressure on each pressure drop value were expressed by very simple equations. These equations can be applied also to CO_2.

4.1 Generalized characteristics of friction pressure drop at supercritical pressure

The friction pressure drop - flow rate characteristics are generalized by the following method. Dimensionless flow rate ξ and dimensionless friction pressure drop ΔP_f^* are defined as follows:

$$\xi \equiv G/G_0, \quad \Delta P_f^* \equiv \Delta P_f/\Delta P_{f0}, \quad \cdots\cdots\cdots (17)$$

where G_0 is a reference flow rate defined as the flow rate at which the fluid assumes a pseudo-critical state at the tube exit at certain values of pressure, heat flux, and inlet enthalpy. ΔP_{f0} is the reference friction pressure drop defined as the friction pressure drop when the flow rate is G_0.

Using the approximated relation for enthalpy and specific volume as shown in Fig.9 and assuming a uniform heat flux and a uniform friction coefficient along the test tube, the generalized expression of friction pressure drop is expressed by

$$\Delta P_f^* = \frac{\xi^2}{1-(br_s/2)(a/b)}\left\{\frac{br_s}{2}\left(1-\frac{b}{a}\right)\xi + (1-br_s) + \frac{br_s}{2}\frac{1}{\xi}\right\}, \quad \cdots\cdots\cdots\cdots (18)$$

where a and b represent the gradient of specific volume vs. enthalpy in preheated and superheated regions respectively(Fig.9), and r_s is defined as

$$r_s = (i_{cp}-i_i)/i_{cp} \quad , \quad \cdots\cdots\cdots\cdots (19)$$

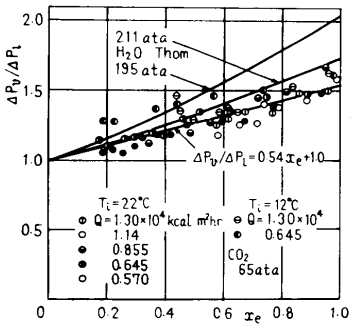

Fig.14 Friction pressure drop ratio

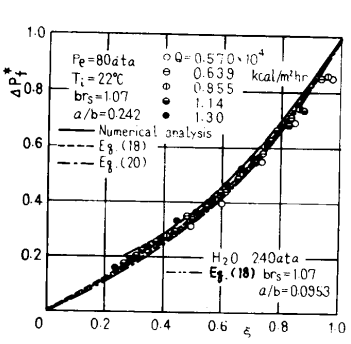

Fig.15 Dimensionless characteristics of friction pressure drop

where i_{cp} is the boundary value between preheated and superheated regions and nearly equal to the pseudo-critical enthalpy. The value of i_{cp} is 148.2 kcal/kg at pressure 80 ata for CO_2. Substitution of a/b=0 that is, constant specific volume in preheated region, into Eq.(18), gives

$$\Delta P_f^* = \xi^2\left\{\frac{br_s}{2}\xi + (1-br_s) + \frac{br_s}{2}\frac{1}{\xi}\right\}. \quad \cdots\cdots (20)$$

It can be seen from Eqs.(18) and (20) that the dimensionless characteristics of friction pressure drop depend on only a/b and br_s independently of the heat flux.

Experimental results of friction pressure drop at P_e=80 ata, T_i=22 °c and 12 °c fall on a single curve independently of heat flux as shown in Figs.15 and 16, and also the calculated results obtained by numerical integration and the results by Eqs.(18) and (20) in these figures. The experimental data, numerically calculated result and these equations agree with each other. Therefore, if an absolute value of friction pressure drop at a certain flow rate is known, the absolute values of the friction pressure drop at other flow rates can be well predicted using the above relations. ΔP_f^*-ξ relation is uniquly determined only by a/b and br_s independently of kinds of fluid as can be seen from Eqs.(18) and (20). The equivalent pressure and inlet enthalpy for water are 240 ata and 445, 422 kcal/kg against the experimental conditions of P_e=80 ata (P/P_{cr}=1.06) and T_i=22, 12 °c (br_s=1.07, 1.5) for CO_2 respectively. The calculated results for water with the above conditions by Eq.(18) are shown in Figs.15 and 16. These curves agree well with those for CO_2, though the values of a/b are different from each other but the effect is very small.

4.2 Generalized characteristics of friction pressure drop at subcritical pressure

The generalized friction pressure drop defined with Eq.(17) in subcritical pressure region in a tube composed of a preheated and an evaporating region is expressed by Eq.(21), and in a tube composed of preheated, an evaporating, and a superheated region is expressed by Eq.(22)

$$\Delta P_f^* = \xi^2\left\{\frac{1}{2}\alpha\frac{r_0}{r}\xi + \left(1-\alpha\frac{r_0}{r}\right) + \frac{1}{2}\alpha\frac{r_0}{r}\frac{1}{\xi}\right\}, \quad \left(1+\frac{r}{r_0}\right)^{-1} \leqq \xi < 1 \quad \cdots\cdots (21)$$

$$\Delta P_f^* = \xi^2\left[\left\{\frac{1}{2}\alpha\frac{r}{r_0} - \alpha\left(1+\frac{r}{r_0}\right) + \frac{1}{2}\left(1+\frac{r}{r_0}\right)^2 \times \frac{r_0}{v'}\frac{dV_{SH}}{dI_{SH}}\right\}\xi + \left\{1+\alpha-\left(1+\frac{r}{r_0}\right)\frac{r_0}{v'}\frac{dV_{SH}}{dI_{SH}}\right\} + \frac{1}{2}\frac{r_0}{v'}\frac{dV_{SH}}{dI_{SH}}\frac{1}{\xi}\right], \quad 0 \leqq \xi \leqq \left(1+\frac{r}{r_0}\right)^{-1} \quad \cdots\cdots (22)$$

where $\alpha = v''/v' - 1$, $r_o = i' - i_i$, $r = i'' - i'$, and dV_{SH}/dI_{SH} is the gradient of specific volume against enthalpy in superheated region.

The experimental results of friction pressure drop at P_e=65 ata agree well with Eqs.(21) and (22) as shown in Fig.17. So the generalized expressions are useful also at the subcritical pressure, and Eqs.(21) and (22) are applicable not only to CO_2 but also to H_2O for the same reason described above.

4.3 Comparison with the previous method of friction pressure drop at supercritical pressure

Prediction methods of the friction pressure drop at supercritical pressure have been reported by Ishigai-Sekoguchi[8] and Shvarts et al.[9] The calculated values by both methods are normalized to get the relationship between ΔP_f^* and ξ, and these are shown in Fig.18, and compared with the results obtained by authors' methods. The conditions used for the calculation are as

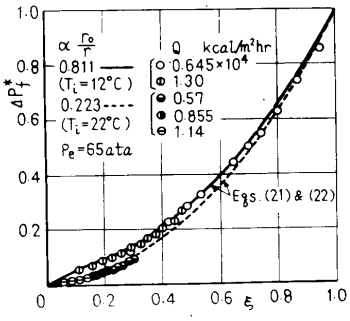

Fig.17 Dimensionless characteristics of friction pressure drop

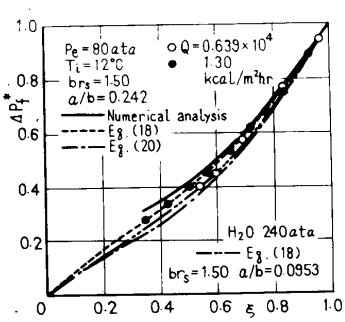

Fig.16 Dimensionless characteristics of friction pressure drop

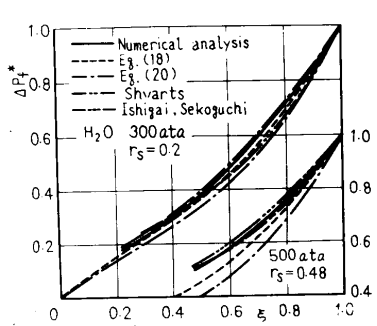

Fig.18 Dimensionless characteristics of friction pressure drop

follows: The working fluid is water, a straight tube of 34.5 mm I.D., and 300 m length, heat flux $Q=3.32\times10^4$kcal/m^{2}h, P_e= 300 ata, r_s=0.2 (i_i=412 kcal/kg), and P_e= 500 ata, r_s=0.48 (i_i=277 kcal/kg). As the friction coefficient in this calculation Itaya's equation (23) is used.

$$\lambda=0.314/\{0.7-1.65\log R_e+(\log R_e)^2\} \quad \cdots\cdots\cdots\cdots (23)$$

It is seen that all curves agree well at low r_s, and Eqs.(18) and (20) give slightly smaller values than those by the other methods at high r_s. The absolute values of the friction pressure drop obtained by these methods differ slightly with each other owing to the difference in the assumptions used. But the normalized characteristics (ΔP_f^*-ξ) for these methods approximately agree with each other.

5. Conclusions

Experimental investigation of friction pressure drop of CO_2 in a long heated tube at supercritical and subcritical pressures are conducted, and the following results are obtained:

1. The friction pressure drop increases monotonously with the flow rate as a curve of second degree at low heat flux, and that changes as a curve of third degree having a point of inflexion at high heat flux.
2. The calculated values of friction pressure drop by the numerical integration method agree well with the experimental results.
3. The mean friction coefficient along the tube is expressed by Eq.(12).
4. Generalized expressions for the friction pressure drop (18), (20), (21), and (22) agree well with the experimental results. This means that the results obtained for CO_2 can be applied to the prediction of the friction pressure drop for H_2O.

Authors wish to express thanks to Prof. Miyabe, Oita University, for his valuable help to provide the data of thermophysical properties of CO_2. Gratitude is extended also to M. Okada, A. Shirasaki, M. Asano, S. Nakai, M. Imoto, and K. Ogura for their assistance in carrying out the experiment, and to all members in Computer Center, Kobe University. A part of the experiment was supported by Fund of Scientific Research, Ministry of Education.

References

(1) Angelino, G., Trans. ASME, Ser. A, 90-3 (1968-7), 287.
(2) White, C.M., Proc. Roy. Soc. Lond., Ser. A, 123 (1929), 645.
(3) Ito, H., Trans. ASME, Ser. D, 81-2 (1959-6), 129.
(4) Ishigai, S., et al., Preprint of Japan Soc. Mech. Engrs. (in Japanese), No. 744-3 (1974-3), 10.
(5) Martinelli, R.C., Nelson, D.B., Trans. ASME, 70-6 (1948-8), 695.
(6) Thom, J.R., Int. J. Heat and Mass Transf., 7-7 (1964-7), 709.
(7) Sakaguchi, T., et al., Memoirs of Engineering, Kobe University, 20 (1974), 143.
(8) Ishigai, S., Sekoguchi, K., Science of Machine (in Japanese), 11-3 (1959), 399.
(9) Shvarts, A.L., et al., Teploenergetika, 15-3 (1968-3), 81.